HYDROLOGICAL PROCESSES
*Hydrol. Process.* (2012)
Published online in Wiley Online Library
(wileyonlinelibrary.com) DOI: 10.1002/hyp.9318

# Evolution of scouring process downstream of grade-control structures under steady and unsteady flows

Jau-Yau Lu,[1]* Jian-Hao Hong,[1] Kai-Po Chang[1] and Tai-Fang Lu[2]

[1] *Department of Civil Engineering, National Chung Hsing University, Taichung, Taiwan*
[2] *Department of Statistics and Informatics Science, Providence University, Taichung, Taiwan*

## Abstract:

For many incised channels, one of the most common strategies is to install some hard structures, such as grade-control structures (GCSs), in the riverbed to resist further incision. In this study, a series of experiments, including both steady and unsteady flow conditions, were conducted to investigate the scouring process downstream of a GCS. Three distinct phases, including the initial, developing and equilibrium phases, during the evolution of scour holes were identified. In addition, a semi-empirical method was proposed to predict the equilibrium scour-hole profile for the scour countermeasure design. In general, the comparisons between the experimental and simulated results are reasonably consistent. As the studies on temporal variation of the scour depth at GCSs caused by floods are limited, the effect of flood hydrograph shapes on the scour downstream of GCSs without upstream sediment supply was also investigated experimentally in this study. Based on the dimensional analysis and the concept of superposition, a methodology is proposed to simulate the time evolution of the maximum scour depth downstream of a GCS for steady flows. Moreover, the proposed scheme predicts reasonably well the temporal variations of the maximum scour depth for unsteady flows with both single and multiple peak. Copyright © 2012 John Wiley & Sons, Ltd.

KEY WORDS grade-control structure; scour; sediment transport; unsteady flows

*Received 3 March 2011; Accepted 16 March 2012*

## INTRODUCTION

Channel incision receives public attention as a result of the impacts on man-made structures and its high repairing or replacement costs. Many civil engineering structures, such as bridges and levees, have been extensively affected by channel incision in Taiwan and also throughout the world. One of the most widely used remedial measures is to install grade-control structures (GCSs) in the river to limit further degradation upstream of the GCSs. However, the GCSs cannot completely solve the incision problem in case of sediment starvation because edge failure may occur downstream of the GCSs and finally damage the GCSs through head cutting.

After a GCS is constructed, initially, the coarser sediment particles are trapped upstream of the GCS, whereas the finer particles may pass through it during floods. The GCSs are usually 1.5–2 m higher than the original riverbed. When the flow passes through a GCS, a critical flow condition may be found immediately upstream of the GCS, whereas a supercritical flow condition can be found on the ramp of the GCS. Downstream of the GCS, an impinging/plunging jet diffuses the energy into the pool. Far downstream of the pool, a uniform flow may occur (Lenzi *et al.*, 2003a).

Scour downstream of a GCS/drop has attracted many researchers to study. Initially, they focused on the geometry of the scour hole, especially for the equilibrium maximum scour depth. Schoklitsch (1932) proposed one of the earliest formulae to predict the scour depth for the flow over a drop based on a flume study. The main parameters in his equation are the unit discharge, the height between head and tailwater level, and $D_{90}$. Schoklitsch (1932) considered the unit discharge and the height difference as parameters related to the impact forces on the bed, and $D_{90}$ as a parameter related to the resistance. After Schoklitsch (1932), many researchers paid a lot of attention to the scouring issue. Mason and Arumugam (1985) and Hoffmans and Verheij (1997) summarized a wide range of empirical equations for predicting the equilibrium maximum scour depths induced by plunging jets. Bormann and Julien (1991) took into account the effect of the jet angle near the water surface on the scour depth downstream of a GCS. However, in these previous studies, a deposit mound was formed downstream of the scour hole because of the horizontal channel slope. No matter whether it is an impinging jet, horizontal jet or plunging jet, if the channel bed slope is very mild, eventually a deposit mound will occur downstream of the scour hole and becomes a boundary condition to arrest the development of the scour hole (Chiew and Lim, 1996).

Considering the effect of channel slope on the scouring processes downstream of bed sills, Gaudio *et al.* (2000) proposed formulae to describe the maximum scour depth and the length of scour hole based on a morphological length and a median particle size. Lenzi *et al.* (2002) extended the research of Gaudio *et al.* (2000) and proposed improved relationships to predict the scour depth and length. In the studies of Gaudio *et al.* (2000) and Lenzi *et al.* (2002), the distance between two bed sills

*Correspondence to: Jau-Yau Lu, Department of Civil Engineering, National Chung-Hsing University, Taichung, Taiwan 40227.
E-mail: jylu@mail.nchu.edu.tw

is long enough for the development of the scour hole. Moreover, Marion *et al.* (2004) investigated the effect of the sill spacing and sediment grading on the potential erosion by jets formed over the sills. They found that decreasing the distance between two sills may lead to the reduction of the scour hole as compared with its potential size. Similar results can also be found in Meftah and Mossa (2006). Both Marion *et al.* (2004) and Pagliara (2007) studied the effect of sediment gradation on scour depth and pointed out that the effect is pronounced for non-uniform sediment.

Many investigations on scour profiles induced by jets have been carried out over the past decades. Chatterjee *et al.* (1994) and Dey and Sarkar (2006) investigated the scour downstream of an apron because of submerged horizontal jets and found that the scour profiles are similar in nature. Pagliara (2007) also proposed a polynomial equation to describe the measured scour profiles. However, Gaudio *et al.* (2000), Lenzi *et al.* (2003a,b), Meftah and Mossa (2006) and Tregnaghi *et al.* (2007) pointed out that scour profiles at equilibrium are affine. To reduce the scour depth and to prevent the failure of the GCS, the hydraulic engineers usually launch riprap or gabions downstream of the GCS. Although it is very useful to know the scale of the scour hole for the adoption of the proper scour countermeasure, only little attention has been placed on the scour-hole profiles downstream of the GCSs under sloping channel conditions.

In natural rivers, severe riverbed scour usually occurs during floods. The unsteady force acting on the riverbed is different from that acted by a steady flow. Breusers and Raudkivi (1991), Hoffmans and Verheij (1997) and Dargahi (2003) showed that many scour phenomena are time dependent and should be investigated in advance.

To date, the time variations in bridge-scour depths have attracted the attention of many researchers (Kothyari *et al.*, 1992; Cardoso and Bettess, 1999; Melville and Chiew, 1999; Mia and Nago, 2003; Chang *et al.*, 2004; Oliveto and Hager, 2005). Oliveto and Hager (2005) also examined their calculating scheme under a multiple-peak hydrograph.

With consideration of the primary horseshoe vortex, sediment pick rate and superposition concepts, Kothyari *et al.* (1992) proposed a semi-empirical model to calculate the time evolution of the maximum pier-scour depth under steady and unsteady flow conditions. Lu *et al.* (2008) modified the method by Kothyari *et al.* (1992) to simulate the variation of pier-scour depths in the field and obtained good agreement with the measured values. Recently, a similar concept was also adopted for the simulation of the temporal variations of scour at non-uniform piers under unsteady flows (Lu *et al.*, 2011).

In contrast to pier scour, little research has been conducted regarding the time evolution of the maximum scour depth downstream of a sill/GCS. Gaudio and Marion (2003) and Dargahi (2003) proposed different time scales for the simulation of the temporal variations of the maximum scour depth. Tregnaghi *et al.* (2009; 2010) investigated the effect of flash floods on the scour at sequence sills with symmetrically triangular-shaped and long flood recession hydrographs, respectively. They provided a methodology to predict the final scour depth downstream of a sill after the occurrence of a flood. Recently, Tregnaghi *et al.* (2011) assumed that at any time, the scour depth evolves at the same rate as in an equivalent steady flow. Based on this assumption, they proposed a model for the simulation of time-varying scouring at bed sills under single-peak hydrograph conditions. However, the scouring process under a multiple-peak hydrograph was not considered.

Furthermore, the effect of incision-related undermining of GCSs tends to occur during high-flow conditions. Based on the field observations and investigations (Water Resources Planning Institute, 2009), it was found that most GCS failures occurred during floods. More research into scour downstream of a GCS is required, especially under unsteady flow conditions.

The present study aims to investigate the development of scour hole in non-cohesive sediment downstream of a GCS. The experimental results are used to develop a semi-empirical model for predicting the equilibrium scour profile. An attempt is also made to calculate the temporal variation of the maximum scour depth downstream of a GCS under both steady and unsteady flows.

## EXPERIMENTAL SETUP AND PROCEDURE

The experiments were carried out in a re-circulating flume 17.5-m long, 0.6-m wide, and 0.6-m deep with glass sidewalls. The flow discharge was controlled by an inlet valve and calibrated by a water tank downstream of the flume. The linear correlation coefficient between the valve opening reading and the flow discharge was 0.998. Figure 1 shows the schematic diagram of experimental arrangement under equilibrium scour conditions. The working length of the flume $L$ that represents the sediment recess was 3.5 m, which was chosen to be large enough to guarantee full scour development with no geometrical interference (Marion *et al.*, 2004). Two types of perspex making the GCS models, with different ramp slopes ($S_{rm} = 0.25$, 0.143) and two uniform sediment sizes ($D_{50} = 2.7$ mm, 3.5 mm), were used for the scouring tests. The head of GCS models $P$ (total drop height) was kept constant ($P = 45$ mm). Eighteen sets of experimental runs under steady flow conditions (Table I), and 32 sets of experiments under unsteady flow conditions (Table II) were performed in this study. As shown in Table I, all the flows belong to subcritical flow. The Froude numbers range from 0.36 to 0.93. The stepwise hydrographs for the unsteady flow conditions, including the advanced, symmetrical and delayed hydrographs, are shown in Figure 2. No sediment was supplied upstream during the experiments. A video camera was attached to the glass sidewall to record the temporal variations of the bed profiles. The video records were then analysed using a digital image processing technique with a precision of 0.3 mm developed by the authors. It had also been tested against point gauge measurements. Reasonably close results were obtained using the two methods. As shown in Figure 1, point B represents the location ($x_{s,me}$) of the maximum equilibrium

 

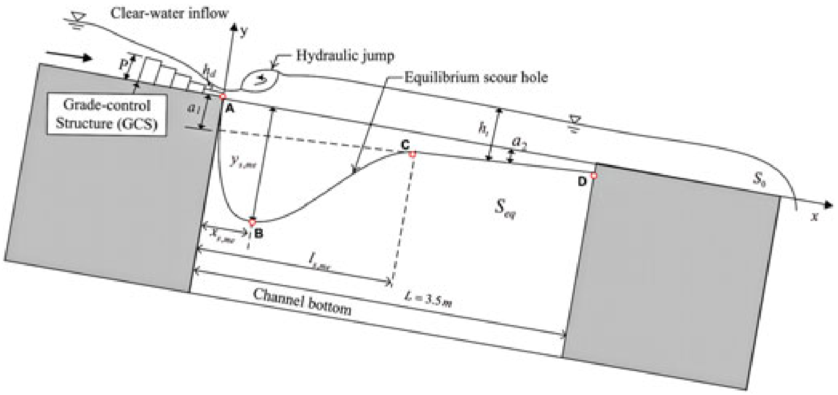


Figure 1. Schematic diagram of scour downstream of a grade-control structure (not to scale)

Table I. Experimental results for steady flow conditions

| Run | $S_b$ | $S_{rm}$ | $D_{50}$ (mm) | $q$ (m$^2$/s) | $F_{dd}$ | $x_{m,e}$ (mm) | $y_{m,e}$ (mm) | $l_{m,e}$ (mm) | $F_r$ |
|---|---|---|---|---|---|---|---|---|---|
| S-M1R4-5 | 0.01 | 0.25 | 3.5 | 0.0167 | 3.50 | 119 | 59 | 450 | 0.81 |
| S-M1R4-8 | 0.01 | 0.25 | 3.5 | 0.0475 | 4.75 | 316 | 136 | 1450 | 0.77 |
| S-M1R7-5 | 0.01 | 0.143 | 3.5 | 0.0167 | 4.12 | 124 | 55 | 470 | 0.93 |
| S-M1R7-8 | 0.01 | 0.143 | 3.5 | 0.0475 | 5.87 | 259 | 129 | 1220 | 0.63 |
| S-M2R4-5 | 0.01 | 0.25 | 2.7 | 0.0167 | 3.62 | 150 | 71 | 683 | 0.56 |
| S-M2R4-8 | 0.01 | 0.25 | 2.7 | 0.0475 | 5.05 | 604 | 151 | 2500 | 0.58 |
| S-M2R7-5 | 0.01 | 0.143 | 2.7 | 0.0167 | 4.43 | 149 | 74 | 700 | 0.85 |
| S-M2R7-6 | 0.01 | 0.143 | 2.7 | 0.0225 | 4.68 | 171 | 95 | 894 | 0.64 |
| S-M2R7-7 | 0.01 | 0.143 | 2.7 | 0.0283 | 5.20 | 337 | 104 | 1087 | 0.61 |
| S-M2R7-8 | 0.01 | 0.143 | 2.7 | 0.0475 | 5.98 | 522 | 152 | 1750 | 0.60 |
| S-S1R4-1 | 0.015 | 0.25 | 3.5 | 0.0167 | 3.05 | 213 | 111 | 888 | 0.67 |
| S-S1R4-4 | 0.015 | 0.25 | 3.5 | 0.0475 | 4.99 | 445 | 204 | 1750 | 0.86 |
| S-S1R7-1 | 0.015 | 0.143 | 3.5 | 0.0167 | 3.05 | 152 | 92 | 532 | 0.54 |
| S-S1R7-4 | 0.015 | 0.143 | 3.5 | 0.0475 | 4.64 | 679 | 241 | 1950 | 0.67 |
| S-S2R4-1 | 0.015 | 0.25 | 2.7 | 0.0167 | 2.85 | 326 | 169 | 857 | 0.41 |
| S-S2R4-4 | 0.015 | 0.25 | 2.7 | 0.0475 | 4.73 | 678 | 246 | 2150 | 0.45 |
| S-S2R7-1 | 0.015 | 0.143 | 2.7 | 0.0167 | 3.19 | 335 | 149 | 1056 | 0.36 |
| S-S2R7-4 | 0.015 | 0.143 | 2.7 | 0.0475 | 4.83 | 836 | 300 | 2150 | 0.53 |

$S_b$ = channel bed slope.
$S_{rm}$ = ramp slope.
$D_{50}$ = median particle size.
$q$ = discharge per unit width.
$F_{dd} = (q/h_d)/(g'D_{50})^{0.5}$, where $g' = [(\rho_s-\rho)/\rho]g$, reduced gravitational acceleration,
$\rho_s$ = sediment density,
$\rho$ = water density,
$g$ = the gravitational acceleration.
$x_{m,e}$ = position of maximum scour depth at the equilibrium stage for steady flows.
$y_{m,e}$ = maximum scour depth at the equilibrium stage for steady flows.
$l_{m,e}$ = maximum scour hole length at the equilibrium stage for steady flows.

Table II. Experimental conditions for unsteady flows

| Run | $S_b$ | $S_{rm}$ | $D_{50}$ (mm) | Type of hydrograph |
|---|---|---|---|---|
| U-S1R7 | 0.015 | 0.143 | 3.5 | (a) ~ (d) |
| U-M1R7 | 0.01 | 0.143 | 3.5 | (a) ~ (d) |
| U-S1R4 | 0.015 | 0.25 | 3.5 | (a) ~ (d) |
| U-M1R4 | 0.01 | 0.25 | 3.5 | (a) ~ (d) |
| U-S2R7 | 0.015 | 0.143 | 2.7 | (a) ~ (d) |
| U-M2R7 | 0.01 | 0.143 | 2.7 | (a) ~ (d) |
| U-S2R4 | 0.015 | 0.25 | 2.7 | (a) ~ (d) |
| U-M2R4 | 0.01 | 0.25 | 2.7 | (a) ~ (d) |

scour depth. The distance from the original bed to point *B* represents the maximum equilibrium scour depth ($y_{s,me}$), and the distance between point *C* and the upstream end corresponds to the length of the maximum equilibrium local scour hole ($l_{s,me}$).

## RESULTS

### *Scouring process*

Based on the study with clear-water inflow, in general, the scouring process downstream of a GCS under steady

 

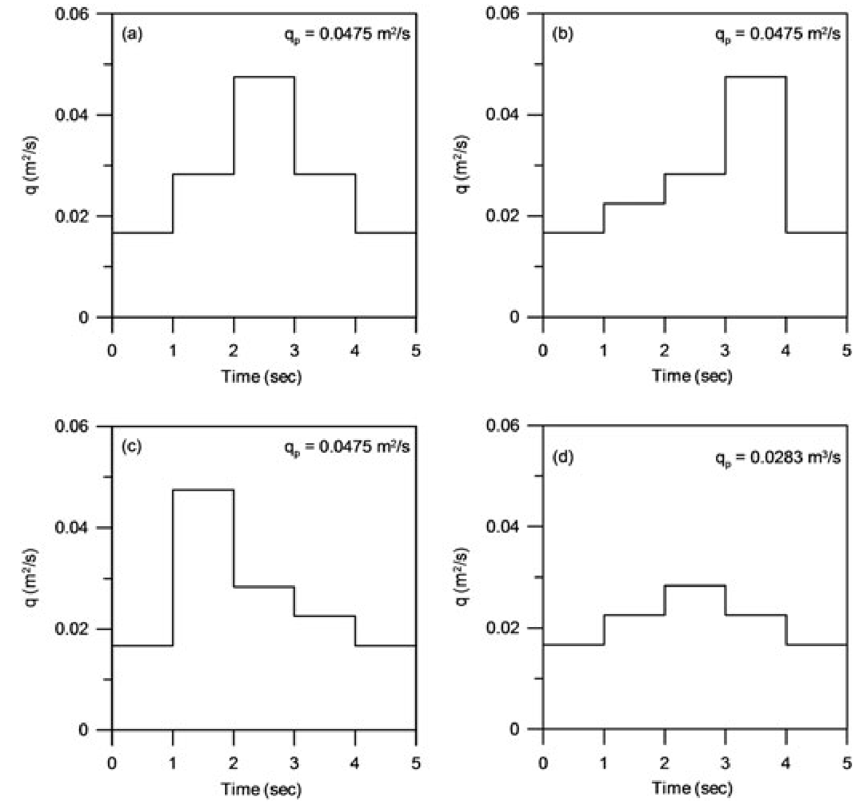


Figure 2. Stepwise hydrographs for the tests under unsteady flow conditions: (a) symmetric; (b) delayed peak; (c) advanced peak; and (d) symmetric, with a lower peak

flow condition can be identified into three distinct phases during the evolution of scour hole, that is, the initial, developing, and equilibrium phases. Figure 3 depicts the typical experimental results for the development of the scour depth as follows:

1. *Phase I (initial stage)*

The movable bed was scoured by the impinging jet induced by the GCS, and a small deposit mound was formed downstream of the scour hole.

2. *Phase II (developing stage)*

The dimension of the scour hole increased with time. The sediment particles oscillated along the downstream slope of the scour hole. Furthermore, the maximum scour depth occurred near the sides of the flume because of the formation of secondary flows in the $x$–$z$ plane induced by the hydraulic jump ($z$ is perpendicular to $x$–$y$ plane in Figure 1).

3. *Phase III (equilibrium stage)*

It can be further identified into three sub-scouring processes. First (Phase III(a)), bursting phenomenon can be found near the location of the maximum scour depth. The scour hole near the GCS was approximately two-dimensional. Second (Phase III(b)), a deposit mound was temporarily formed on the downstream slope of the scour hole because of the accumulation of the falling sediment particles entrained by the impinging jet. During this period, the hydraulic jump occurred very close to the GCS. The impinging jet was somehow restrained by the hydraulic jump, and the location of the maximum scour depth moved slightly upstream. Finally (Phase III(c)), the hydraulic jump gradually moved downstream. The impinging jet was not restrained by the hydraulic jump any more, and the deposit mound vanished gradually. During the equilibrium stage, the scouring process followed the cycle (a)–(c) of Phase III. The bursting phenomenon decreased with time, and the scour hole almost remained unchanged. Finally, the maximum scour depth occurred near the sides of the flume.

*Scour hole dimensions at equilibrium stage under steady flows*

The placement of an armor layer downstream of a GCS, such as rock riprap and rock gabions, is one of the most widely used countermeasures to protect the structure from erosion or edge failure. The estimation of the geometric parameters of the scour hole, including the position ($x_{s,me}$, $y_{s,me}$) of the maximum equilibrium scour depth and the length of the scour hole ($l_{s,me}$), is required for the proper design of the countermeasures. Farhoudi and Smith (1985) and Dey and Sarkar (2006) found that the sediment size and tailwater depth $h_t$ affect the scour depth downstream of a spillway apron. Based on the experimental data, Dey and Sarkar (2006) and Pagliara (2007) reported that the densimetric Froude number had great effect on the scour depth downstream of an apron because of submerged horizontal jets and block ramps, respectively. However, the experiments performed by

 

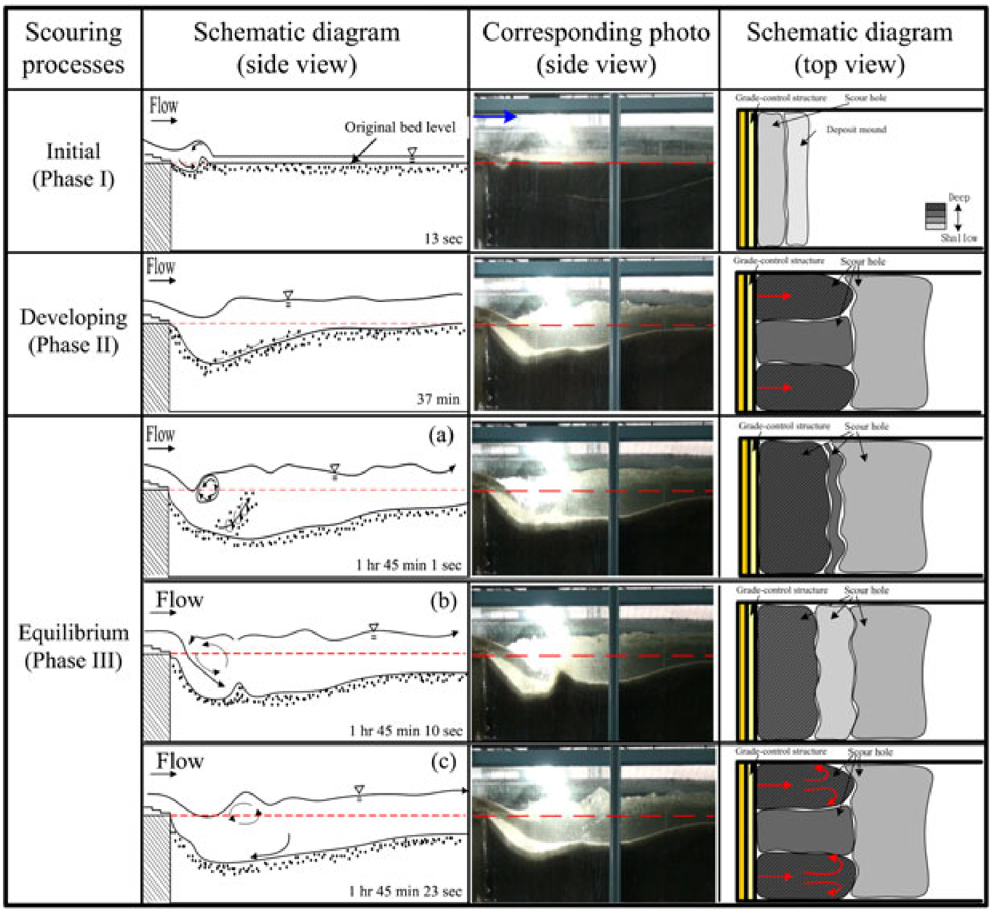


Figure 3. Schematic diagrams of scouring process downstream of a grade-control structure under a typical steady flow condition

Dey and Sarkar (2006) and Pagliara (2007) were under horizontal bed slope conditions. In this study, the experiments were conducted with different bed slopes (Table I). With consideration of the findings by Farhoudi and Smith (1985), Dey and Sarkar (2006) and Pagliara (2007) and incorporating the effect of bed slope, regression analysis for the experimental data (Table I) yielded the following dimensionless equations for the geometric parameters of the scour hole ($x_{s,me}$, $y_{s,me}$, $l_{s,me}$)

$$x_{s,me}/P = 38.9S_b^{1.263}F_{dd}^{0.887}(h_t/D_{50})^{0.867} \tag{1}$$

$$y_{s,me}/P = 351.3S_b^{1.667}F_{dd}^{0.759}(h_t/D_{50})^{0.494} \tag{2}$$

$$l_{s,me}/P = 11.3S_b^{0.595}F_{dd}^{0.812}(h_t/D_{50})^{0.761} \tag{3}$$

Figure 4 shows the comparisons of the measured and predicted scour hole parameters. The $R^2$ values for Equations (1) ~ (3) are 0.86, 0.93, and 0.81, respectively, indicating that Equations (1) ~ (3) correspond satisfactorily with the experimental data. Physically, Equations (1) ~ (3) show that the locus of the maximum scour depth or scour length increases with an increase in channel slope $S_b$, densimetric Froude number $F_{dd}$, or tailwater depth $h_t$, and a decrease in bed material median size $d_{50}$. In fact, a dimensional analysis can be performed to prove the validity of the functional forms of Equations (1) ~ (3).

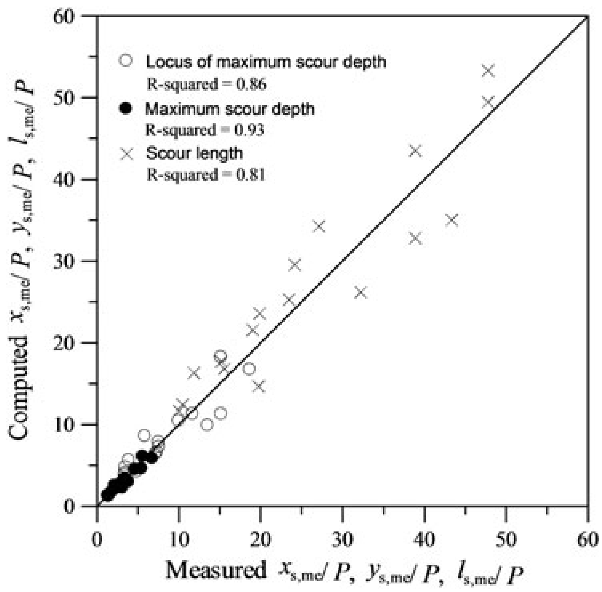


Figure 4. Comparisons of the measured and computed dimensionless geometric parameters ($x_{s,me}$, $y_{s,me}$, $l_{s,me}$) for scour holes

A comparison of the scour depths predicted by Lenzi *et al.* (2002), Marion *et al.* (2004) and Equation (2), and our measured data was also made. As expected, Equation (2), in general, gave the best predictions. The performance of the equation by Marion *et al*. (2004) was slightly better than that of Lenzi *et al*. (2002). No empirical equation for the prediction of scour hole length was derived in the study by Marion *et al*. (2004). A comparison of the scour hole lengths predicted by Lenzi *et al*. (2002) and Equation (3) and our measured data indicated that both equations gave fair predictions.

*Scour hole profiles at equilibrium stage under steady flows*

Dumped riprap and rock gabions are the most common scour countermeasures to minimize the scour depth downstream of a GCS. In this section, a semi-empirical model is proposed to predict the scour-hole profile. Accordingly, river engineers can design the scour countermeasures more economically. Define $X = x_s/l_{s,me}$ and $Y = y_s/y_{s,me}$, where the longitudinal and vertical coordinates $x_s$ and $y_s$ for describing the scour hole are measured with respect to the origin A in Figure 1. Based on the analysis of the existing data [Gaudio and Marion, 2003; Meftah and Mossa, 2006] and those collected in this study, the dimensionless scour-hole profile can be described by

$$\frac{y_s}{y_{s,me}} = C_0 \exp\left(C_1 \frac{x_s}{l_{s,me}}\right)\left[1 - \exp\left(C_2 \frac{x_s U_*}{v}\right)\right] \quad (4)$$

where $C_0$, $C_1$, and $C_2$ are empirical coefficients; $U_* = \sqrt{g h_t S_{eq}}$ ; g = gravitational acceleration; $h_t$= tailwater depth; $v$= kinematic viscousity. The coefficients $C_0$, $C_1$, and $C_2$ are determined using the scour-hole characteristics, which are as follows: (i) at $x_s = x_{s,me}$, $y_s/y_{s,me} = 1$; (ii) at $x_s = x_{s,me}$, $dy_s/dx_s = 0$; and (iii) at $x_s = l_{s,me}$, $y_s = a_2$, where $a_2$= equilibrium general scour depth in reach CD (Figure 1), which can be estimated as follows based on Gaudio and Marion (2003):

$$a_2 = h_t - h_c = \frac{(nq)^{6/7}}{(\theta_c \Delta D_{50})^{3/7}} - \left(\frac{q^2}{g}\right)^{1/3}, \quad \text{for } a_2/h_t > 0.15 \quad (5a)$$

$$q = \frac{2}{3}\sqrt{2g}\left(0.605 + \frac{0.001}{h_t - a_2} + 0.08\frac{h_t - a_2}{a_2}\right)(h_t - a_2)^{3/2}, \quad \text{for } a_2/h_t \leq 0.15 \quad (5b)$$

where n = Manning's roughness coefficient; $\theta_c$ =critical Shields' mobility parameter $= h_t S_{eq}/(\Delta D_{50})$ for wide channels; $S_{eq}$ = equilibrium bed slope downstream of the maximum scour depth; $\Delta$ = relative submerged particle density = $(\rho_s - \rho_w)/\rho_w$; $\rho_s$ = density of sediment particles; and $\rho_w$ =density of water; $q$ = water discharge per unit width. Using the pre-mentioned three boundary conditions, one can obtain three equations. The empirical coefficients $C_0$, $C_1$, and $C_2$, can then be determined by solving the simultaneous nonlinear equations.

The scour-hole profiles computed using the presented method are compared with the observed experimental data in several typical cases as shown in Figures 5(a)–(h). In general, the proposed method predicts the experimental data with bed slope $S_b$= 0.015 better than those with $S_b$ = 0.01. It is because the undulant variations occurred on the lower slope ($S_b$ = 0.01), although this phenomenon gradually disappeared on the higher slope ($S_b$ = 0.015), especially with higher flow discharges or smaller median sediment size, for example, Figure 5(h).

Figure 6 shows the comparisons of the results obtained from the proposed model with the experimental data of Meftah and Mossa (2006). The model predicts the scour-hole profiles between the origin and the maximum scour depth very well but slightly overestimates the scour depths for reach beyond the maximum scour depth. Overall, however, the model predicts the scour-hole profiles quite reasonably.

*Temporal variation of maximum scour depth–steady flow conditions*

The time variation of scour downstream of a GCS because of plunging jet was tested for uniform sediment with different sizes (Table I). According to the experimental observations, the scour depth $y_{s,t}$ at time $t$ can be expressed as a function of tailwater depth ($h_t$), densimetric Froude number, time, and channel slope as follows:

$$y_{s,t}/y_{s,me} = f(S_b, F_{dd}, T) \quad (6)$$

where $T = t/t_R$; $t_R$ = reference time = $h_t/(g' D_{50})^{0.5}$; $g' = \Delta g$. The dimensionless maximum scour depth $y_{s,t}/y_{s,me}$ can be expressed as an exponential function of $T$ as follows:

$$y_{s,t}/y_{s,me} = 1 - \exp\left(-b_0 \times T^{b_1}\right) \quad (7)$$

where $b_o = 0.0468$ and $b_1 = 0.421$ are coefficients determined by using SPSS. The coefficient of determination $R^2$ for Equation (7) is 0.95. As shown in Figure 7, all the data collapse in a narrow band. Although there are some discrepancies between the measured and predicted results at the initial stage of scour activity, the model, in general, predicts the temporal variations of scour depths downstream of a bed sill under steady flow conditions satisfactorily.

*Evolution of maximum scour depth–single-peak hydrograph*

Tregnaghi *et al*. (2009, 2010) had performed a series of experiments on scour downstream of uniformly spaced bed sills with uniform sediment under both symmetrical and asymmetrical hydrographs. The time variations of the maximum scour depth during floods were investigated and fitted with polynomial equations. In the present study, a semi-empirical model is proposed for calculating the time variations of scour at a GCS under unsteady flow conditions based on the concept of superposition. Figure 8

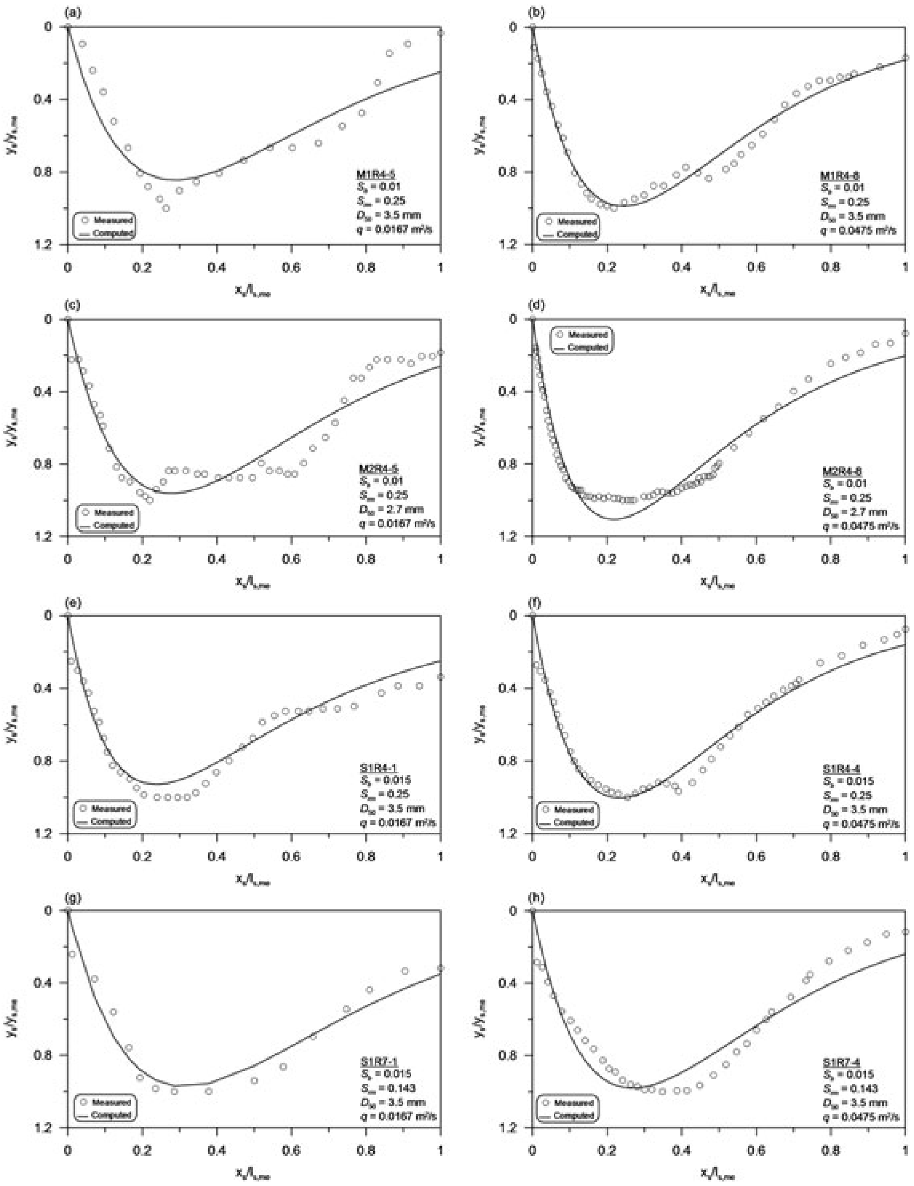


Figure 5. Comparisons of the observed (circle) and predicted (curve) scour-hole profiles under steady flow conditions for runs: (a) M1R4-5, (b) M1R4-8, (c) M2R4-5, (d) M2R4-8, (e) S1R4-1, (f) S1R4-4, (g) S1R7-1 and (h) S1R7-4

shows the schematic diagram of the model. A stepwise hydrograph consisting of the rising ($Q_1 \sim Q_3$) and recession ($Q_4$) limbs as depicted in Figure 8(a) is used to illustrate the procedure.

Chatterjee *et al*. (1994), Dey and Sakar (2006) and Pagliara (2007) found that the scour hole shapes downstream of a GCS and cross-river hydraulic structure are similar in nature. Meftah and Mossa (2006) also found that if the spacing between two GCSs is long enough, the shapes of scour holes are also similar. In Figure 3, during the initial stage (only a few seconds), a deposit mound was temporarily formed downstream of the GCS and gradually washed away by the flow. However, one can see in the figure that the shapes of scour holes are fairly similar during the developing and equilibrium phases. Based on this finding, we assume that the concept of superposition can be applied to most of the scouring processes except for the very initial stage under unsteady flow conditions. As the initial stage is very short, it would not affect the calculation significantly.

Figure 8(b) shows the time variation of scour depth at a GCS for different steady flow rates ($Q_j$, $j = 1$, 2, 3 and 4). The specific steps for computing the scour depth at a GCS under an unsteady flow are given below:

1. For the first flow rate $Q_1$, the time evolution of scour depth follows the $y_s$ curve of $Q_1$ [i.e. $O'A'$, as shown in Figure 8(b)]. The corresponding scour depth is $y_{s,\ 1}$.
2. As the flow rate increases from $Q_1$ to $Q_2$ at time $t_1$, the temporal variation of scour depth follows the path $A''B'$ of $y_s$ curve corresponding to $Q_2$. Because $Q_2 > Q_1$, the time required for the scour depth to reach $y_{s,1}$ for the flow rate $Q_2$ is less than $t_1$. This time is designated as $t_1^*$ in Figure 8(b).
3. When the flow rate increases from $Q_2$ to $Q_3(> Q_2)$ at $t = t_1^* + (t_2 - t_1)$, the $y_s$curve follows the path $B''C'$of the

 

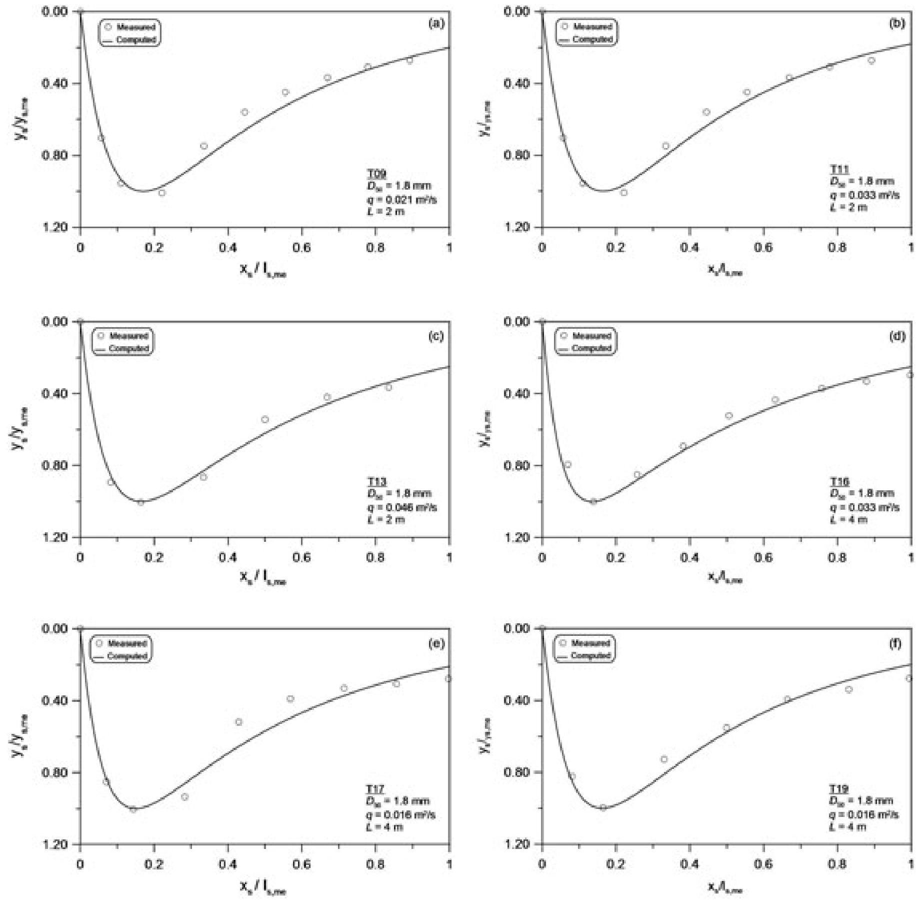


Figure 6. Comparisons of the scour-hole profiles predicted by the proposed method with the experimental data of Meftah and Mossa (2006)

scour depth curve for $Q_3$. Because $Q_3 > Q_2$, the time required for the scour depth to reach $y_{s,2}$ for the flow rate $Q_3$ is less than$t_2$. This time is designated as $t_2^*$ in Figure 8(b).

4. However, at time $t_3$, as the flow rate decreases from $Q_3$ to $Q_4$ corresponding to $t = t_2^* + (t_3 - t_2)$, the scour depth may remain unchanged, that is, $y_{s,3} = y_{s,4}$. On the other hand, if the slope of the recession limb is mild, the scouring potential of $Q_4$ may cause further scour, which means $y_{s,4}$ may be slightly greater than $y_{s,3}$. Furthermore, for the steep recession limb, the scour depth remains unchanged because of the reduced stream power. The $y_s$ curve may follow the path$C''D'$ of the scour depth curve for $Q_4$.

*Determination of time lag $t_i^*$*

To determine the time lag $t_i^*$, Equation (7) for the temporal variation of the scour depth at a sill under steady flow conditions is adopted.

Considering the stepwise discharges $Q_1$ and $Q_2$ ($> Q_1$), $Q_1$ lasts a period of $t_1$, whereas the subsequent $Q_2$ lasts a period of $(t_2 - t_1)$. The time evolution of the scour depth for $Q_1$ is determined by

$$\frac{y_{s,m}(t_1)}{y_{s,me1}} = 1 - \exp\left\{-b_0 \cdot \left[\frac{t_1 \left(g' D_{50}\right)^{1/2}}{h_{t,1}}\right]^{b_1}\right\} \tag{8}$$

For the stepwise discharge $Q_2$, the scour depth *versus* time can be expressed as

$$\frac{y_{s,m}(t_1^*)}{y_{s,me2}} = 1 - \exp\left\{-b_0 \cdot \left[\frac{t_1^* \left(g' D_{50}\right)^{1/2}}{h_{t,2}}\right]^{b_1}\right\} \tag{9}$$

As shown in Figure 8(b), one can obtain $t_1^*$ based on Equations (8) and (9) by letting $y_{s,m}(t_1) = y_{s,m}(t_1^*)$, that is,

$$t_1^* = \frac{h_{t,2}}{\left(g' D_{50}\right)^{1/2}} \left\{\frac{1}{-b_0} \ln\left[\left(y_{s,me2} - y_{s,me1} + y_{s,me1} \cdot \exp\left(-b_0 \cdot \left(\frac{t_1 \left(g' D_{50}\right)^{1/2}}{h_{t,1}}\right)^{b_1}\right)\right) \Big/ y_{s,me2}\right]\right\}^{\frac{1}{b_1}} \tag{10}$$

 

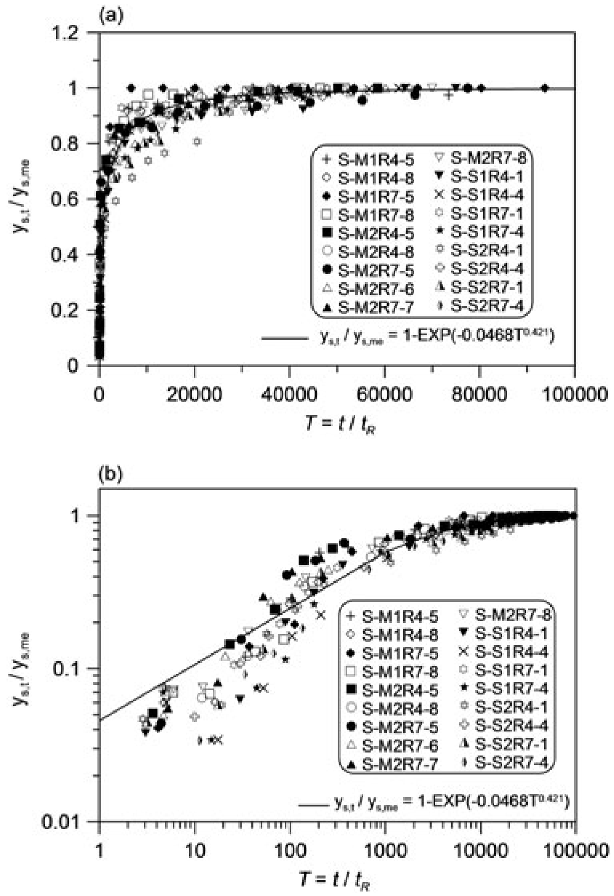


Figure 7. Dimensionless temporal variations of maximum scour depth under steady flow conditions

As the flow rate increases from $Q_2$ to $Q_3$, one can use similar concept to determine $t_2^*$, that is,

$$t_2^* = \frac{h_{t,3}}{\left(g' D_{50}\right)^{1/2}} \cdot \left\{ \frac{1}{-b_0} \ln \left[ \left( y_{s,me3} - y_{s,me2} + y_{s,me2} \cdot \exp\left( -b_0 \cdot \left( \frac{\left(t_1^* + t_2 - t_1\right)\left(g' D_{50}\right)^{1/2}}{h_{t,2}} \right)^{b_1} \right) \right) \Big/ y_{s,me3} \right] \right\}^{\frac{1}{b_1}} \tag{11}$$

It should be noted that when $t_i^*$ is less than zero, $y_{s,\,i+1} = y_{s,\,i}$, and the scour depth will not increase with time.

The same procedure continues for the remaining steps of the hydrograph.

Experiments on the scour depth evolution under stepwise hydrograph without upstream sediment supply were carried out as summarized in Table II. Figure 9 shows the time evolution of the scour depth under stepwise hydrographs with single-peak flow conditions. For the stepwise hydrographs with the same peak flow and duration [Figures 9(a) ~ (c)], the experimental results show that the maximum scour depths are almost the same. Interestingly, the time for the occurrence of the maximum scour depth highly correlates with the type of the hydrographs. For example, the maximum scour depth occurs earlier for the advanced hydrograph than the delayed one. For the same duration with different peak flows as shown in Figures 7(d) and 9(a), the maximum scour depth increases with an increase in the peak flow. In general, the proposed model simulates the time evolution of the scour depth downstream of a GCS under single-peak flood conditions reasonably well. It can be seen that the scour depth is slightly reduced after the flood peak, which is resulted from the collapse of the sediment particles near the downstream edge of the GCS. The falling sediment may slightly reduce the scour depth.

*Multiple-peak hydrograph*

During the natural flood events, the multiple-peak hydrographs occur frequently. The proposed model is used to simulate the scour under unsteady flow with a multiple-peak hydrograph. Figure 10 shows a comparison of the simulated and measured scour depth evolutions under a multiple-peak flow hydrograph. The second peak of the hydrograph is larger than the first one in this case. As shown in Figure 10, in the first portion of the hydrograph, the maximum scour depth occurs at the first

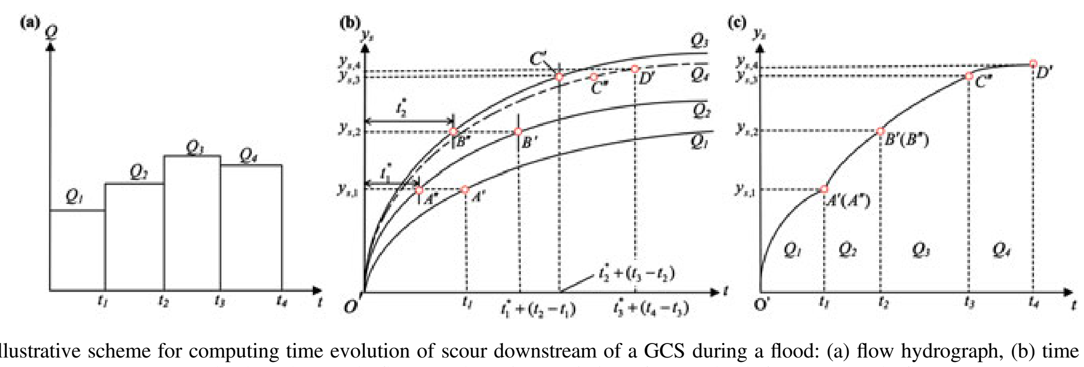

Figure 8. Illustrative scheme for computing time evolution of scour downstream of a GCS during a flood: (a) flow hydrograph, (b) time variations of scour depth under steady flows, and (c) time variation of scour depth for an unsteady flow

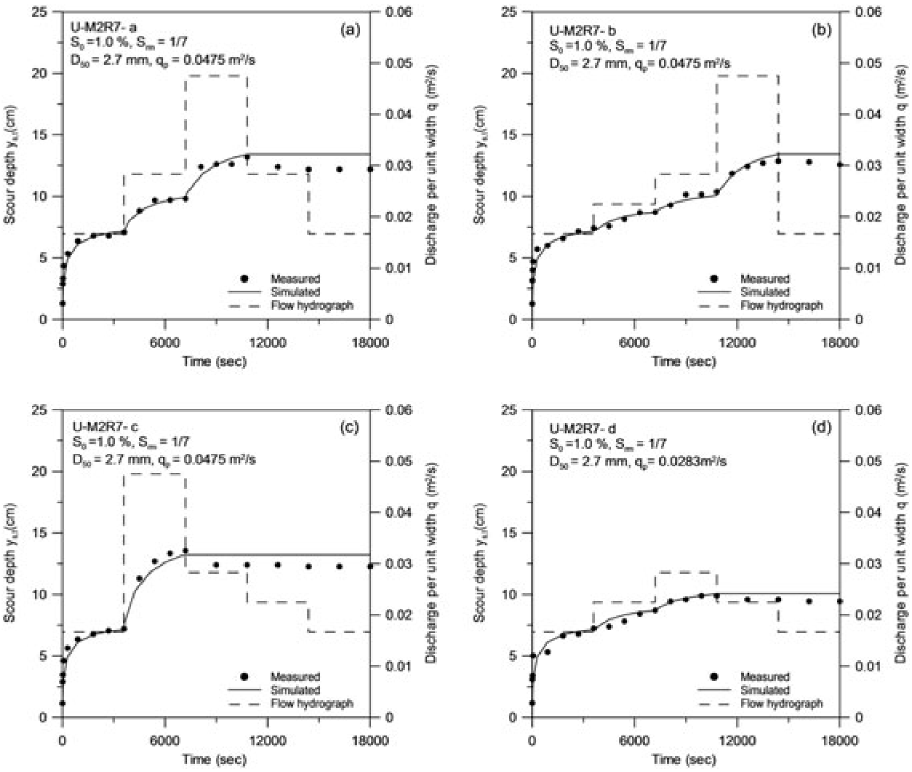


Figure 9. Simulated and measured scour depth evolutions under stepwise hydrographs with single peaks: (a) symmetric, $q_p = 0.0475\,\mathrm{m^3/s}$, (b) delayed peak, (c) advanced peak, (d) symmetric, $q_p = 0.0283\,\mathrm{m^3/s}$

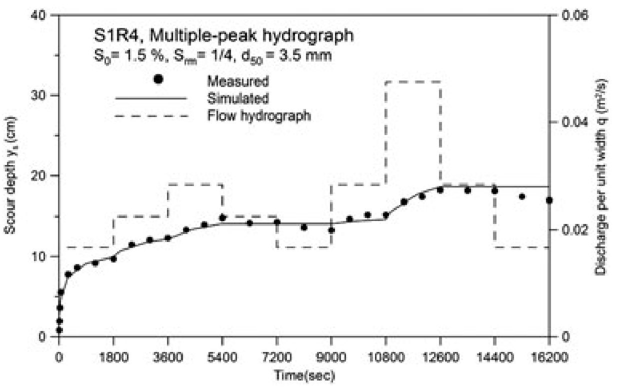


Figure 10. Simulated and measured scour depth evolutions under a stepped hydrograph with multiple peak

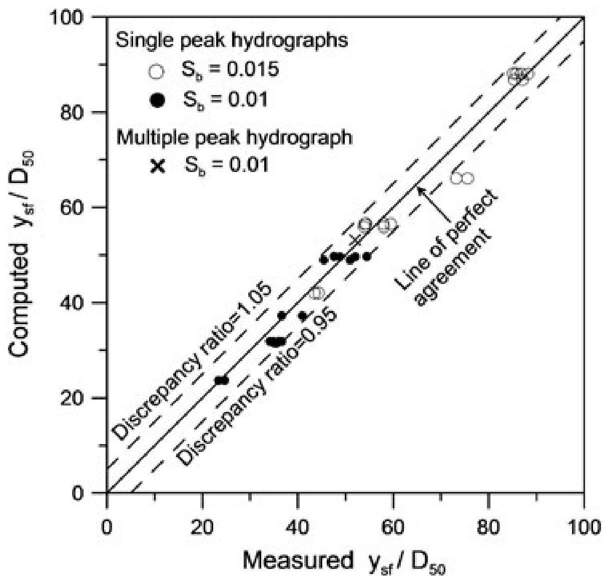


Figure 11. Comparison between the calculated and measured final maximum scour depths under stepped hydrographs

peak ($t = 5400$ s). In the second portion of the hydrograph ($t > 9000$ sec), the scour depth initially increases slowly. However, it increases rapidly near the second peak ($t = 10\,800 \sim 12\,600$ s) because the second peak ($q_{p2} = 0.0475\,\mathrm{m^2/s}$) is much greater than the first ($q_{p1} = 0.0283\,\mathrm{m^2/s}$). Similar to the results for the single-peak hydrograph, the scour depths are also slightly reduced after the two peaks. However, for the practical purpose, the maximum scour depth is of major concern, and the proposed scheme gives reasonably accurate predictions.

*Prediction of maximum scour depth after unsteady flows*

Figure 11 shows a comparison of the predicted and measured final maximum scour depths under unsteady flow conditions. The dashed lines give the ±5% error interval, whereas the solid line is the perfect agreement line. In general, the proposed prediction procedure gives less than ±5% error for all of the data, including the single-peak and multiple-peak hydrographs. Only two data points are outside the interval, indicating the prediction is fairly satisfactory. In reality, most of the coarse sediment particles are trapped upstream of the GCS, whereas only a slight amount of them can be carried downstream by the flush flow during floods. The fine particles may not have significant effect on reducing the scour depth downstream of the GCS. For a single flood event, the discharge hydrograph usually can be approximately represented by a stepped hydrograph, and the scour depth downstream of the GCS can be computed by the proposed scheme. However, the proposed scheme is under the condition without sediment supply upstream of the GCS. As a result, the computed scour depth tends to be conservative and on the safety side.

## CONCLUSIONS

Experiments on scour downstream of a GCS because of flood events were investigated with two uniform sediments without upstream sediment supply for various ramp slopes, channel slopes and flow hydrographs. The proposed method is proved to be a useful tool for the analysis of the problems involving plunging jet scour induced by floods. Based on the experimental results and the analysis of the scour downstream of a GCS, the main findings of the study are summarized as follows:

1. According to the experimental observations, the hydraulic jump formed downstream of a GCS-induced large secondary flows and the vortices (*x*–*y* plane), resulting in the occurrence of the maximum scour depths near the side walls.
2. Empirical formulae are derived to quantify the maximum scour depth, the scour length, and the location of the maximum scour depth downstream of a GCS under steady flow conditions. The equilibrium scour hole dimensions ($x_{s,me}$, $y_{s,me}$, $l_{s,me}$) increase with an increase in the channel slope, densimetric Froude number, and tailwater depth and a decrease in the median sediment size.
3. The equilibrium scour-hole profile downstream of a GCS for steady flows can be estimated based on an exponential function with three boundary conditions. The comparison between the experimental data and the predicted values gives good agreement.
4. The dimensionless maximum scour depth for steady flows can be expressed as an exponential function of the dimensionless time $T$. The empirical equation predicts the temporal variation of the maximum scour depth reasonably well.
5. Based on the dimensional analysis and the concept of superposition, a scheme is proposed to estimate the temporal variation of the maximum scour depth downstream of a GCS under unsteady flow conditions.

### ACKNOWLEDGEMENTS

This study was supported by the National Science Council of the Republic of China. The writers gratefully acknowledge Mr Zhong-Zhi Shi's help and Prof. Rajkumar V. Raikar's valuable suggestions.

### REFERENCES

Bormann NE, Julien PY. 1991. Scour downstream of grade-control structures. *Journal of Hydraulic Engineering* **117**(5): 579–594.

Breusers HNC, Raudkivi AJ. 1991. *Scouring*. Hydraulic structures design manual, A. A. Balkema, Rotterdam, The Netherlands.

Cardoso AH, Bettess R. 1999. Effects of time and channel geometry on scour at bridge abutments. *Journal of Hydraulic Engineering*, **125**(4): 388–399.

Chang WY, Lai JS, Yen CL. 2004. Evolution of scour depth at circular bridge piers. *Journal of Hydraulic Engineering* **130**(9): 905–913.

Chatterjee SS, Ghosh SN, Chatterjee M. 1994. Local scour due to submerged horizontal jet. *Journal of Hydraulic Engineering*, **120**(8): 973–992.

Chiew YM, Lim SY. 1996. Local scour by a deeply submerged horizontal circular jet. *Journal of Hydraulic Engineering* **122**(9): 529–532.

Dargahi B. 2003. Scour development downstream of a spillway. *Journal of Hydraulic Research* **41**(4): 417–426.

Dey S, Sarkar A. 2006. Scour downstream of an apron due to submerged horizontal jets. *Journal of Hydraulic Engineering* **132**(3): 246–257.

Farhoudi J, Smith KVH. 1985. Local scour profiles downstream of hydraulic jump. *Journal of Hydraulic Research* **23**(4): 343–358.

Gaudio R, Marion A. 2003. Time evolution of scouring downstream of bed sills. *Journal of Hydraulic Research* **41**(3): 271–284.

Gaudio R, Marion A, Bovolin V. 2000. Morphological effects of bed sills in degrading rivers. *Journal of Hydraulic Research* **38**(2): 89–95.

Hoffmans GJCM, Verheij HJ. 1997. *Scour Manual*. Hydraulic structures design manual, A. A. Balkema, Rotterdam, The Netherlands.

Kothyari UC, Garde RCJ, Ranga Raju KG. 1992. Temporal variation of scour around circular bridge piers. *Journal of Hydraulic Engineering* **118**(8): 1091–1106.

Lenzi MA, Marion A, Comiti F. 2003a. Interference processes on scouring at bed sills. *Earth Surface Processes and Landforms* **28**(1): 99–110.

Lenzi MA, Marion A, Comiti F. 2003b. Local scouring at grade-control structures in alluvial mountain rivers. *Water Resources Research* **39**(7): 1176–1188.

Lenzi MA, Marion A, Comiti F, Gaudio R. 2002. Local scouring in low and high gradient streams at bed sills, *Journal of Hydraulic Research* **40**(6): 731–739.

Lu JY, Hong JH, Su CC, Wang CY, Lai JS. 2008. Field Measurements and Simulation of Bridge Scour Depth Variations during Floods. *Journal of Hydraulic Engineering* **134**(6): 810–821.

Lu JY, Shi ZZ, Hong JH, Lee JJ, Raikar RV. 2011. Temporal Variation of Scour Depth at Nonuniform Cylindrical Piers. *Journal of Hydraulic Engineering* **137**(1): 45–56.

Marion A, Lenzi MA, Comiti F. 2004. Effect of sill spacing and sediment size grading on scouring at grade-control structures. *Earth Surface Processes and Landforms* **29**(8): 983–993.

Mason PJ, Arumugam K. 1985. Free jet scour below dams and flip buckets. *Journal of Hydraulic Engineering* **111**(2): 220–235.

Meftah MB, Mossa M. 2006. Scour holes downstream of bed sills in low-gradient channels *Journal of Hydraulic Research* **44**(4): 497–509.

Melville BW, Chiew YM. 1999. Time scale for local scour at bridge piers. *Journal of Hydraulic Engineering* **125**(1): 59–65.

Mia MF, Nago H. 2003. Design method of time-dependent local scour at circular bridge pier. *Journal of Hydraulic Engineering* **129**(6): 420–427.

Oliveto G, Hager WH. 2005. Further results to time-dependent local scour at bridge elements. *Journal of Hydraulic Engineering* **131**(2): 97–105.

Pagliara S. 2007. Influence of sediment gradation on scour downstream of block ramps. *Journal of Hydraulic Engineering* **33**(11): 1241–1248.

Schoklitsch A. 1932. *Kolkbidung unter uberfallstrahlen*. Die Wasserwirtschaft.

Tregnaghi M, Marion A, Bottacin-Busolin A, Tait S. 2011. Modelling time varying scouring at bed sills. *Earth Surface Processes and Landforms* **36**(13): 1761–1769.

Tregnaghi M, Marion A, Coleman S. 2009. Scouring at bed sills as a response to flash floods. *Journal of Hydraulic Engineering* **135**(6): 466–475.

Tregnaghi M, Marion A, Coleman S, Tait SJ. 2010. Effect of flood recession on scouring at bed sills. *Journal of Hydraulic Engineering* **136**(4): 204–213.

Tregnaghi M, Marion A, Gaudio R. 2007. Affinity and similarity of local scour holes at bed sills. *Water Resources Research* **43**: W11417. DOI: 10.1029/2006WR005559

Water Resources Planning Institute. 2009. *Investigation of failure mechanism and new scour countermeasures at grade-control structures (2/2)*. Water Resources Agency: Taiwan, R.O.C. (in Chinese).

 